Hyperfine interaction mediated exciton spin relaxation in (In,Ga)As quantum dots

H. Kurtze,[1] D. R. Yakovlev,[1] D. Reuter,[2] A. D. Wieck,[2] and M. Bayer[1]
[1]*Experimentelle Physik 2, Technische Universität Dortmund, D-44221 Dortmund, Germany*
[2]*Angewandte Festkörperphysik, Ruhr-Universität Bochum, D-44780 Bochum, Germany*
(Received 6 February 2012; published 4 May 2012)

The population dynamics of dark and bright excitons in (In,Ga)As/GaAs quantum dots is studied by two-color pump-probe spectroscopy in an external magnetic field. With the field applied in Faraday geometry and at $T < 20$ K, the dark excitons decay on a ten nanoseconds time scale unless the magnetic field induces a resonance with a bright exciton state. At these crossings their effective lifetime is drastically shortened due to spin flips of either electron or hole by which the dark excitons are converted into bright ones. Due to the quasielastic character we attribute the origin of these flips to the hyperfine interaction with the lattice nuclei. We compare the exciton spin relaxation times in the two resonances and find that the spin flip involving an electron is approximately 25 times faster than the one of the hole. A temperature increase leads to a considerable, nonmonotonic decrease of the dark exciton lifetime. Here phonon-mediated spin flips due to the spin-orbit interaction gradually become more important.

DOI: 10.1103/PhysRevB.85.195303 PACS number(s): 78.55.Cr, 78.67.Hc

I. INTRODUCTION

The spin dynamics in quantum dots (QDs) have attracted considerable interest recently as they strongly differ from the dynamics observed in systems of higher dimensionality.[1] For QD-confined carriers the spin-orbit (SO) interaction and the hyperfine (HF) interaction have been identified as relevant factors for these dynamics.[2–7] The relaxation processes can be characterized by the longitudinal relaxation time (T_1) and the transversal relaxation time (T_2).[8] T_1 describes the relaxation between the spin states split by an external magnetic field, while T_2 describes the damping of the precessional motion about the magnetic field. Here we focus on T_1-relevant scattering processes.

Relaxation processes induced by the two prime mechanisms for spin scattering carry different characteristics: Due to the small nuclear Zeeman splitting in the sub-μeV range flip-flop processes with carrier spins mediated by the HF interaction are quasielastic so that they require quasidegeneracy of the involved carrier spin levels. By contrast SO-mediated scattering events involve acoustic phonons which have substantial density of states and significant interaction matrix elements at larger splittings in the order of a meV.

The consequences of these characteristics have been studied so far mainly for single QD-confined carriers, electrons or holes. At $B = 0$ the SO interaction is inefficient for carriers in the degenerate ground state Kramers doublet, leading to spin relaxation times up to milliseconds at cryogenic temperatures.[2,9–11] When applying a sufficiently strong magnetic field, though, phonon-induced relaxation can be strongly enhanced, leading to a dramatic shortening of T_1. Otherwise, as long as the field-induced Zeeman energy is comparable to the nuclear spin splitting, the HF interaction is the dominating relaxation mechanism.[12,13]

The situation is distinctly different for charge-neutral excitons, which are the focus of interest here. For them the electron-hole exchange interaction leads to a finite energy splitting between bright and dark excitons (details below), so that phonon-mediated relaxation may occur already at zero magnetic field.[14–16]

The importance of the HF interaction for exciton complexes is not so clear yet. For bright excitons, which couple to the light field, the lifetime of about a nanosecond is shorter than the time during which this interaction can act efficiently. Dark excitons have considerably longer lifetime up to microseconds, and hence were investigated recently with respect to potential applications in quantum information.[17,18] Especially for them the HF interaction might become relevant.

Generally, the HF interaction can be decomposed into three contributions: (1) the Fermi-contact interaction, (2) the magnetic dipole-dipole interaction, and (3) the orbital momentum coupling to the nuclei.[19] These interactions have to be evaluated for the wave functions of an electron in the conduction band or a hole in the valence band. The conduction band in zinc-blende semiconductors is formed by *s*-type orbitals, so that only interaction (1) is important for electrons, while the other two terms vanish when evaluating the corresponding matrix elements.

In contrast to these findings for the conduction band, the HF interaction of holes has been thought to be much weaker, if not negligible: The *p*-type Bloch function results in a vanishing carrier density at the nuclear sites. If so, the holes might have relaxation times exceeding those of the electrons.[20–22] However, recent theoretical works have gone beyond the simplification down to the Fermi-contact terms and have shown that the anisotropic parts of the HF interaction may contribute significantly to the hole spin dynamics. The hyperfine interaction strength between a hole spin and the nuclear spins may be comparable to the electron hyperfine interaction, depending on the valence band structure of the QD ground state which is determined by strain and confinement.[19,23] If the valence band ground state contains light-hole admixtures, the interaction Hamiltonian is not of Ising type any longer and hole spin flips become possible. Very recent studies have validated these estimations and have shown that the ratio of the hole and electron HF interaction strength is on the order of 0.1.[17,18,24,25]

In this paper we study the spin relaxation in self-assembled In(Ga)As/GaAs QDs. By means of magnetic fields we tune

the exciton fine structure into resonances where quasielastic spin flips can take place between dark and bright ground-state excitons. For the low-temperature regime, the spin flips are initiated by the HF interaction where the nuclei serve as scattering partners. The exciton conversions require a spin flip of either an electron or a hole. Our results show that we can separate these two flip-flop processes so that we can distinguish quantitatively between the electron HF interaction strength and that of a hole. Spin relaxation processes due to the SO interaction are also examined.

II. EXPERIMENTAL TECHNIQUE AND SAMPLE CHARACTERIZATION

The spin dynamics addressed here is distinctly different from that in QDs charged only by a single carrier species because of the energy level structure: A ground state exciton is formed by an electron with spin $S_{e,z} = \pm 1/2$ and a hole with $J_{h,z} = \pm 3/2$, assuming pure heavy hole character. The exchange interaction couples the electron and the hole spin, resulting in total angular momentum projections $M = S_{e,z} + J_{h,z} = \pm 1$ and ± 2 which correspond to bright and dark excitons, respectively. These states are split by the isotropic exchange δ_0.

For the dots under study, the δ_0 splitting amounts to $\approx$100 μeV which would have to be released for spin flips between the two exciton reservoirs. Applying a magnetic field induces a Zeeman splitting of the bright and the dark excitons so that resonances between dark and bright exciton states can occur at particular longitudinal fields [as seen also in the scheme in Fig. 1(a)].

The experiments are performed by a two-color pump-probe technique using two synchronized, independently wavelength-tunable Ti:sapphire lasers. The lasers emit linearly polarized pulses of 1.5 ps duration at a repetition rate of 75.6 MHz. The temporal jitter between the two pulse trains is well below 1 ps. We use one laser as a pump which excites carriers nonresonantly in the GaAs barrier. The other probe laser is used to test the exciton population in the QD ground state. The nonresonant pump excitation ensures that spin relaxation occurs during relaxation of carriers into their ground states (characterized by a time scale on the order of 10 ps). Therefore quantum dots capturing an electron-hole pair can contain exciton spin configurations that are bright or dark.

The temporal delay Δt between pump and probe is adjusted by a micrometer-precise mechanical delay line. The resulting time-resolved differential transmission (DT) signal is detected by a pair of balanced Si photodiodes connected to a lock-in amplifier, by which we take the difference between the probe beam sent through the sample with and without pump action. The pump excitation density into the GaAs barrier at 1.55 eV photon energy is $I_0 = 10\ \mathrm{W/cm^2}$. The probe density is chosen to be ten times weaker at an energy matching the center of the QD ground state emission band (1.37 eV). At the used pump densities we detect basically only QD ground state emission in photoluminescence (PL), limiting the number of electron-hole pairs per dot to a maximum of two. Comparing emission spectra for different excitation powers shows further that the average exciton occupation per QD is well below unity at the applied pump power, as the ground state emission intensity is less than half of its saturation level.

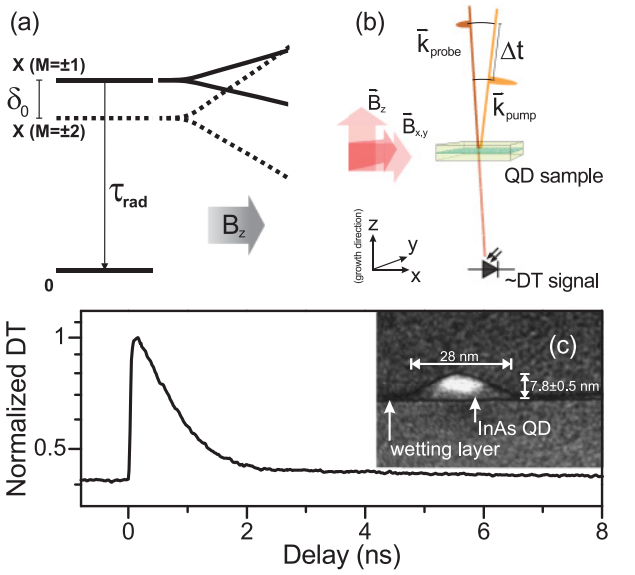

FIG. 1. (Color online) (a) Level diagram of bright (angular momentum $M = \pm 1$) and dark ($M = \pm 2$) excitons for the QDs under study, subject to an external magnetic field B_z along the QD growth direction. δ_0 denotes the (isotropic) exchange interaction energy; τ_{rad} is the radiative decay time. (b) Sketch of the experimental configuration as described in the text. (c) Time-resolved DT trace, observed for a pump (probe) excitation density of $I_0 = 10\ \mathrm{W/cm^2}$ ($1\ \mathrm{W/cm^2}$) at $T = 10$ K. Note the $\log_{10}$ scale for the vertical axis. The inset gives a cross-sectional transmission electron micrograph image of an unannealed self-assembled InGaAs/GaAs QD, nominally identical to the as-grown QDs in this work.

Figure 1(b) shows a sketch of the experimental configuration. We apply magnetic fields $B \leqslant 7$ T either in the longitudinal Faraday configuration (parallel to the sample growth direction and the optical axis **z**) or in the transverse Voigt configuration (perpendicular to **z**). The fields are generated by an optical split-coil magnetocryostat. The QD sample under study is placed in the variable temperature insert of the cryostat which allows us to lower the temperature down to 5 K.

The heterostucture was grown by molecular beam epitaxy and contains 10 layers of nominally undoped (In,Ga)As/GaAs QDs, separated from each other by 100-nm-wide barriers. To get an idea of the dot geometry, a QD sample was studied by high-resolution transmission electron microscopy [see inset in Fig. 1(c)]. From this micrograph we estimate the dot dimensions to be about 8 nm in height and 30 nm in diameter. The structure was exposed to postgrowth rapid thermal annealing (RTA, 30 seconds at 920 °C), leading to interdiffusion of dot and barrier material and enhancing the QD volume. As a result the QD emission is shifted into the sensitivity range of the used Si detectors.

Figure 1(c) shows a typical DT trace at $T = 10$ K. The nonresonant pump excitation at $\Delta t = 0$ excites carriers which quickly relax to the dot ground state leading to a fast rise of the DT signal on a 10 ps time scale. The subsequent time evolution shows two components decaying on different time scales. The first component shows a fast drop with 0.4 ns time constant. We

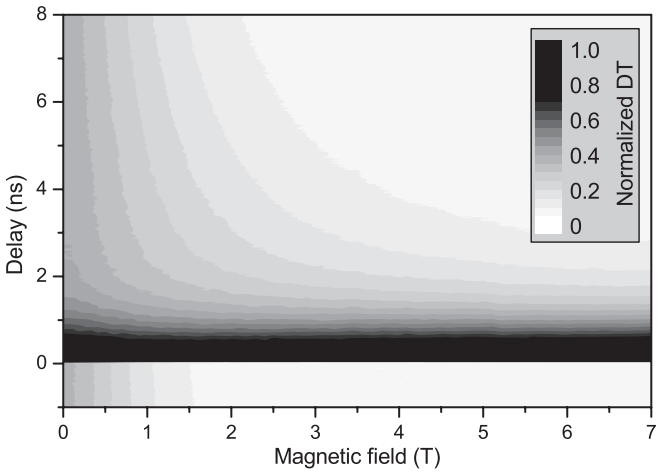

FIG. 2. Contour plot of DT traces (along the vertical axis) vs applied magnetic field in Voigt configuration ($\mathbf{B} \perp \mathbf{z}$, along the horizontal axis). $T = 10$ K, I_0 pump power.

attribute it to bright exciton decay, as the same time is observed for the emission decay τ_{rad} in time-resolved PL (not shown). The slow component decays on times of about 6 ± 1 ns, so that a fraction of this population is still present when the next pump pulse hits the sample (DT > 0 for negative delays). Therefore we associate this population with dark excitons formed by spin flips while relaxing toward the QD ground state after excitation.

III. EXPERIMENTAL RESULTS

The experimental results are presented and discussed in the following order: First we analyze exciton spin relaxations by the DT evolution under transverse and longitudinal magnetic fields (subsections A and B, respectively). Next, we weigh up the HF and the SO interaction at different temperature regimes (C). Finally the results on the spin relaxation due to the HF interaction are examined and discussed (D).

A. Exciton spin relaxation in transverse magnetic fields

The experiments in Voigt configuration confirm our bright and dark exciton assignment made above. In transverse magnetic fields the dark excitons are mixed with the bright excitons, as the rotational symmetry about the growth axis is broken so that the oscillator strength is distributed among the four exciton states.[26] This leads to an enhanced decay rate of the dark excitons. The mixing is the stronger the higher the applied magnetic field is and consequently the dark exciton population decreases with increasing B. The DT data as shown in Fig. 2 reflect this process. The contour plot consists of DT traces (along the vertical axis) as function of the applied Voigt field strength (horizontal scale) up to 7 T, recorded in steps of 0.2 T. The DT amplitude due to the dark exciton population at larger delays Δt decreases smoothly with increasing magnetic field, and for field strengths exceeding $\sim$5 T has basically vanished completely.

B. Exciton spin relaxation in longitudinal magnetic fields

Let us now focus on studies in longitudinal magnetic fields. Following the notations in Ref. 27, the exciton fine structure is given by the effective spin Hamiltonian:

$$\mathcal{H}_X = \mu_B \left(g_{e,z} S_{e,z} + \frac{g_{h,z}}{3} J_{h,z} \right) B - \frac{2}{3} \delta_0 S_{e,z} J_{h,z}, \quad (1)$$

where μ_B is the Bohr magneton and the $g_{e,z}$ and $g_{h,z}$ are the electron and hole g factors along $\mathbf{z}$. The anisotropic exchange splittings of the bright excitons (typically denoted by the energy δ_1) and of the dark excitons (δ_2) are neglected here because $\delta_0 \gg \delta_1, \delta_2$; see Ref. 28.

Equivalent QDs to the ones studied in this work were investigated recently by pump-probe Faraday rotation spectroscopy to determine the parameters of the exciton fine structure Hamiltonian with high accuracy. Besides the exchange interaction $\delta_0 = 100 \pm 10$ μeV, also the electron and hole longitudinal g factors of $g_{e,z} = -0.61$ and $g_{h,z} = -0.45$ were measured.[27] We plot the resulting exciton fine structure splitting as a function of the magnetic field B_z in Fig. 3, panel (a).

The longitudinal field configuration does not break the rotational symmetry so that the exciton angular momentum M remains a good quantum number. The B-linear splitting of bright and dark excitons leads to two crossings in the magnetic field dispersion: The energy dispersion of the $|-2\rangle$ exciton (consisting of a spin-down hole and a spin-down electron, represented by $\Downarrow$ and $\downarrow$, respectively) crosses that of the $|-1\rangle$ exciton ($\Downarrow$ $\uparrow$) around 3 T. It also crosses the $|+1\rangle$ exciton ($\Uparrow$ $\downarrow$) at approximately 4 T.

Figure 3(b) shows a contour plot of DT transients as a function of magnetic field ($T = 10$ K and excitation power I_0). At low fields $B_z < 1$ T the signal shows the two-component behavior already discussed in relation with Fig. 1, panel (c). After pump action the fast bright population decay is followed by the significantly slower dark exciton decay. For increasing fields up to about 3 T, however, the slow decay component shortens which results in decreasing DT amplitudes for longer delays Δt. It increases again reaching times almost as long as at zero field for even higher fields beyond 6 T.

The center of the resonance almost exactly occurs at the field strength at which the crossing of the $|-2\rangle$ exciton with the $|-1\rangle$ exciton was calculated. Hence the field-resonant reduction of the dark exciton population is attributed to a quasiresonant spin-flip process. Here dark excitons are converted into bright excitons and vice versa leading to reduced long-delay DT values compared to those at $B = 0$.[29] If the B_z-dependent fine structure splitting contained a single coincidence, one would expect the resonance to be symmetric with respect to the crossing point. However, in experiment we find a clear asymmetry toward higher B. This asymmetry may indicate that there is another spin-flip resonance at the crossing point of the $|-2\rangle$ exciton with the $|+1\rangle$ exciton.

To analyze this asymmetry in more detail, the inset in Fig. 3(c) shows DT values for a fixed time period vs magnetic field. In order to concentrate on the dark excitons, the time window was chosen to be as late as possible at negative delays $\Delta t < 0$ right before the pump pulse action. The duration of the averaged period is 150 ps to achieve a good signal-to-noise ratio. Besides the clearly resolved resonances, a continuous

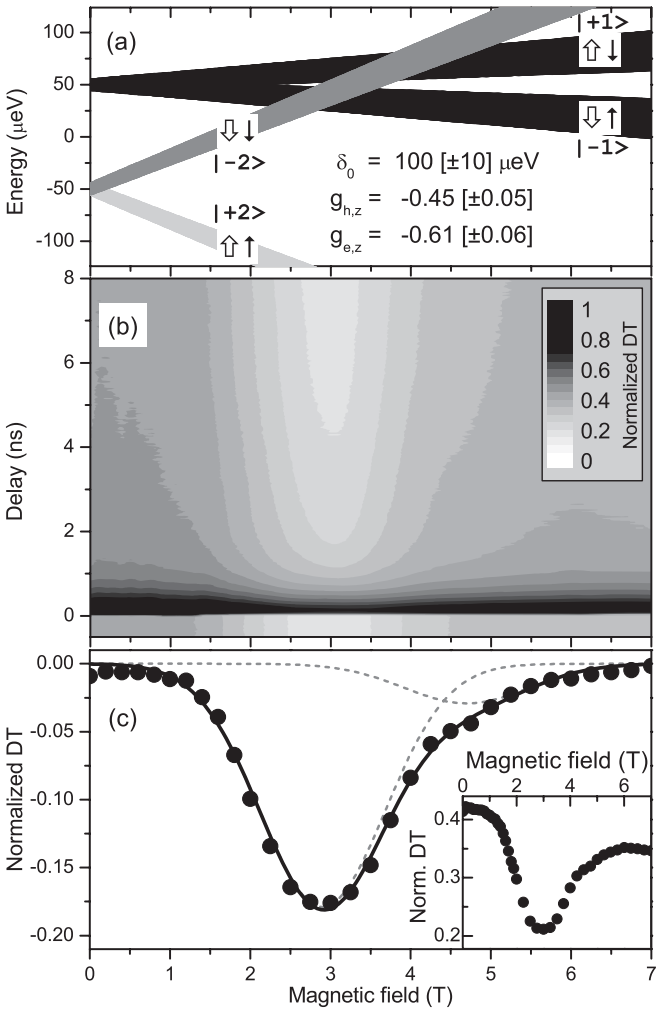

FIG. 3. (a) Fine structure of bright and dark exciton states in the studied QDs subject to a longitudinal magnetic field. The arrows represent the exciton spin configurations where the electron spins $S_{e,z} = +1/2$ and $-1/2$ are symbolized by thin arrows pointing up and down, respectively. The thick arrows give the corresponding orientations of the hole spin $J_{h,z} = \pm 3/2$. (b) Contour plot of DT traces vs Faraday magnetic field strength. $T = 10$ K, pump power I_0. (c) Dots: DT values from (b), averaged over a delay time interval of 150 ps before pump arrival vs magnetic field. The dots in the main panel (inset) show DT values with (without) a baseline subtraction. The solid line is a fit to the DT data by two Gaussians, both of 1.56 T width for each resonance, with each Gaussian shown by the dashed lines.

reduction can be seen which is most likely related to $|+2\rangle$ excitons. These excitons decay faster with increasing B due to increasing energy separation and increasing phonon density which demonstrates that the SO interaction is effective also for low temperatures (see below). In the main panel the resulting data set is baseline subtracted in order to remove the smooth variation of the dark exciton lifetime with magnetic field and to focus fully on the resonances. Values below zero indicate a field-induced reduction of the dark exciton population. Besides the main resonance at 2.9 T, a shoulder is observed toward higher magnetic fields, supporting that indeed two field resonances occur. We fit the data with a superposition of two Gaussians each with a half width of 1.56 T. The Gaussian form is justified by the inhomogeneous broadening of the fine structure parameters in the QD ensemble. The data can be well described by this fit as shown by the solid line. The two dashed curves give the individual resonances. Within the experimental accuracy, the field position of 4.7 T for the weak resonance is in accord with the crossing point of the $|-2\rangle$ and $|+1\rangle$ excitons in Fig. 3(a) (the thickness of the lines reflects the experimental variation of the fine structure parameters).

C. Estimation of the relevant spin relaxation mechanism

The influence of SO-induced spin flips on the exciton evolution is limited at low temperatures: In the single-phonon case a phonon would be absorbed to transfer a dark exciton into a bright one. In perturbation theory the corresponding transition rate is given by (a) the magnitude of the matrix element, (b) the phonon density of states, and (c) the phonon occupation.[30,31] In our case the $|-2\rangle$ exciton comes into resonance with the bright excitons. Though the thermal occupation will be sufficient at $T = 10$ K, the matrix element and the phonon density of states is about zero due to the small energy splitting resulting in inefficient scattering by SO processes. However, we see an effective lifetime reduction of the dark excitons in the experiment. By contrast the $|+2\rangle$ exciton linearly increases its energy separation from the bright excitons corresponding to increasing matrix elements and phonon densities. Here a smooth variation of the SO-related exciton spin relaxation with magnetic field is expected, but a contribution to the observed resonances should be excluded.

In principle also two-phonon scattering (virtual or real via higher orbitals) may become involved. Such scattering processes were shown to be quite efficient, in particular as they do not require nonzero Zeeman splittings.[2,6,16,21,32–34] However, also these processes cannot account for resonances at particular magnetic fields. Moreover, for real transitions the population of phonon modes that bridge excited QD-exciton states is negligible at $T = 10$ K.

The relative importance of the HF and the SO interaction, however, can be altered by increasing the temperature. Especially real two-phonon scattering processes are expected to contribute at thermal energies significantly higher than $T = 10$ K. Here the SO interaction might dominate the relevant exciton spin relaxations and as a consequence the HF-related resonances could vanish in experiment.

Experimental findings confirm these expectations. Figure 4(a) shows a contour plot made up of DT transients at temperatures between $T = 5$ K and $T = 180$ K. For low temperatures $T < 20$ K the DT transients reveal the two-component character that was discussed above in relation with Fig. 1(c). In general with increasing temperatures the difference between the two temporal components tends to fade out and the DT amplitudes for longer delays decrease. However there is a discontinuous behavior in between around 50 K where DT amplitudes for longer delays are less pronounced than at the transients at $T = 30$ and 70 K.

We analyze the experimental DT data with a rate equation that models the exciton population. Since the transition rates from the energetically higher lying bright $M = \pm 1$ excitons to the lower lying dark $M = \pm 2$ will not differ much from the

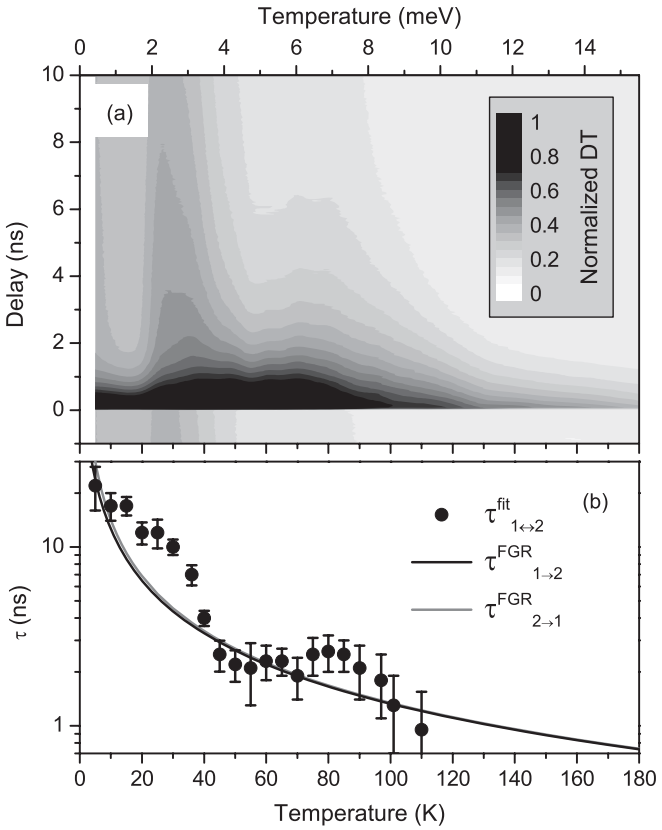

FIG. 4. (a) Contour plot of normalized DT traces for varying temperatures from 5 K to 180 K; $B = 0$, excitation power I_0. (b) The data points give relaxation times $\tau^{\text{fit}}_{1\leftrightarrow 2}$ obtained from a fit to the DT data set from panel (a). Solid lines show calculated single-phonon relaxation times from $M = \pm 1$ to $M = \pm 2$ excitons (and vice versa) as described in the text ($\log_{10}$ scale).

reverse process at these temperatures, we assume a single spin relaxation time $\tau^{\text{fit}}_{1\leftrightarrow 2}$ which serves as a fit parameter. (Details are shown in the Appendix.) The resulting evolution was fitted to each DT transient from Fig. 4(a), and the corresponding relaxation times $\tau^{\text{fit}}_{1\leftrightarrow 2}$ are given by the dots in panel (b). The spin-flip times reduce strongly with increasing temperature starting with ≈20 ns for $T = 5$ K down to ≈1 ns for 110 K. Beyond that the exciton conversion time shows a plateau between $T = 40$ K and 80 K where $\tau^{\text{fit}}_{1\leftrightarrow 2}$ takes on values of approximately 2 ns.

If the underlying spin relaxation mechanism was solely SO-mediated single-phonon scattering, the flip times could simply be described by Fermi's golden rule (FGR).[30,31] For comparison, we compute these flip times $\tau^{\text{FGR}}_{1\to 2}$ and $\tau^{\text{FGR}}_{2\to 1}$ and plot them as solid lines in panel (b) of Fig. 4. (Details again in the Appendix.) These one-phonon relaxation times follow the temperature-dependent phonon occupation N and roughly describe the experimental data. However the results also reveal deviations which indicate spin flips assisted by resonant two-phonon scattering. Here the spin flips involve excitations to higher QD orbitals so that spin relaxation is possible beyond a distinct thermal activation energy while it is blocked below. Apparently, exciton spin scattering processes are additionally enabled around thermal energies of 4 meV (equivalent to $T \approx 40$ K; see upper scale of Fig. 4) which

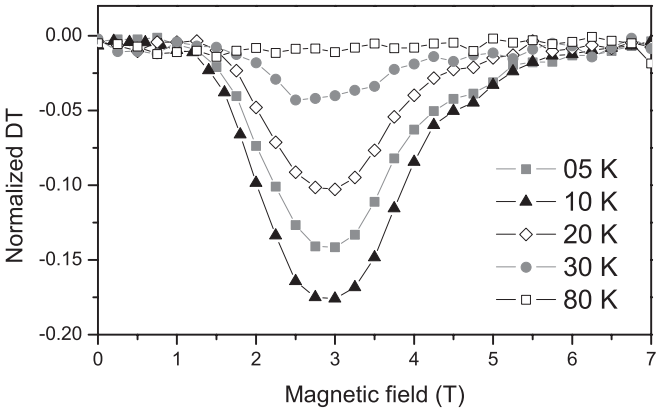

FIG. 5. DT averaged over a negative delay time interval of 150 ps before pump arrival vs magnetic field for various temperatures as indicated. The data are baseline subtracted as in Fig. 3(c).

corresponds to quantization energies of holes in the valence band.[35]

In fact the SO interaction is the primary exciton spin relaxation mechanism at higher temperatures: Fig. 5 gives similar data to those of Fig. 3(c) but for other temperatures. The field-induced resonances show weak variations at low cryogenic temperatures ($T = 5$ K to 20 K; small variations in the amplitude could occur due to changes in the generation of initial dark exciton populations). But already for $T = 30$ K the curve shows only relics of the HF-induced resonances. For even higher temperatures the dark excitons are strongly reduced so that the DT curve lacks any magnetic field dependent resonances (DT curve for 80 K).

D. Examination of HF-mediated exciton spin relaxation times

Let us now evaluate the HF-mediated spin-flip times that become relevant when driving the system into the fine-structure determined resonances at low temperatures, $T = 10$ K. We consider spin conversions between the bright $M = \pm 1$ and the dark $M = -2$ excitons. They are taken into account by spin-flip times $\tau^{\text{fit}}_{-2\leftrightarrow\pm 1}$ which serve as a fit parameter to the experimental DT evolution in the set of coupled rate equations mentioned in the section above [other parameters remain unchanged compared to those in relation with Fig. 4(b)]. Figure 6 compares the experimental DT traces [panel (a)] with the exciton evolution modeled by the rate equations [panel (b)].

At $B = 0$ the exciton populations decay as discussed already above for the undisturbed case [panel (a)]. In comparison the initial decay slows down whereas the decay at longer times becomes faster in the resonances. This behavior is reproduced by the modeled exciton populations [panel (b)]: Right after pump action nonzero spin flip rates convert a fraction of the bright excitons into $|-2\rangle$ excitons by which the fast decay is delayed. For longer delays Δt, $|-2\rangle$ excitons may undergo spin flips into the bright spin configurations. This is followed by a radiative decay which leads to a reduction of the exciton population compared to the off-resonant case. These changes are most obvious in the case of the electron spin flip at $B = 3$ T where $\tau^{\text{fit}}_{-2\leftrightarrow -1} \approx (0.8 \pm 0.15)$ ns is obtained from the fit. In contrast, the spin-flip time due to a hole flip at

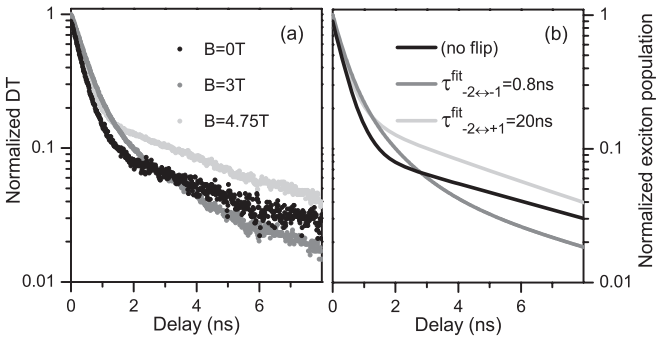

FIG. 6. (a) Normalized DT values vs delay time at field amplitudes of $B = 0$, 3 T, and 4.7 T in Faraday configuration (scattered dots). The traces were set to zero at $\Delta t = 0$. (b) Total exciton population as modeled by a set of rate equations; see text. The numbers give the different values of the parameter τ^{fit} mapping the spin flip of the involved $M = -2$ dark excitons into ± 1 bright ones and vice versa. (Both panels $\log_{10}$ scale.)

$B = 4.7$ T is found to be approximately 25 times slower with $\tau^{\text{fit}}_{-2\leftrightarrow+1} \approx (20 \pm 4)$ ns.

In the remaining part we examine the HF-mediated spin flip scattering events. In the dominant resonance at $B = 3$ T excitons are converted into each other where the electron spin $\mathbf{S}_e$ interacts with one of the nuclei $\mathbf{I}_i$. This corresponds to an effective Hamiltonian given by

$$\mathcal{H}_e = \sum_i A_i |\Psi(\mathbf{r}_{ei})|^2 \mathbf{S}_e \mathbf{I}_i, \tag{2}$$

where the sum goes over all nuclei in the QD electron localization volume. The interaction strength of the electron spin ($\mathbf{S}_e$) with a nucleus ($\mathbf{I}_i$) is determined by the hyperfine constant A_i specific for each nuclear species in the dot and the electron density $|\Psi(\mathbf{r}_{ei})|^2$ at the nuclear site $\mathbf{r}_{ei}$.

The second weaker resonance can be initiated by a hole spin flip only. A dipole-dipole interaction could not convert pure $\pm 3/2$ heavy-hole states into each other due to the mismatch of angular momentum exchange. If it was a pure heavy hole state, the interaction would be described by an Ising-form,

$$\mathcal{H}_h = v_0 \sum_i C_i |\Phi(\mathbf{r}_{hi})|^2 J_{h,z} I_{i,z}, \tag{3}$$

where the $J_{h,z}$ are the hole spin projections along the growth axis, the C_i are the interaction constants, and $|\Phi(\mathbf{r}_{hi})|^2$ is the hole density at a particular nuclear site.

But in the studied QDs the in-plane hole g factor differs considerably from zero, $g_{h,\perp} = 0.15$.[27] This indicates that the hole ground state contains admixtures of light-hole states $\Phi_{\pm 1/2}$ with $J_{h,z} = \pm 1/2$ and the mixed hole states are $\tilde{\Phi}_{\pm 3/2} = (\Phi_{\pm 3/2} + \beta \Phi_{\mp 1/2})/\sqrt{1 + |\beta|^2}$ with the complex mixing coefficient β. Now hole-nuclei flip flops become possible and the two resonances can be treated analogously. The interaction Hamiltonians of the two carrier types with a single nucleus i can be rewritten as

$$\mathcal{H}_{e,i} = \frac{v_0}{2} A_i |\Psi(\mathbf{r}_{ei})|^2 \times \left(\frac{1}{2}(S_{e,+} I_{i,-}) + \frac{1}{2}(S_{e,-} I_{i,+}) + S_{e,z} I_{i,z} \right) \tag{4}$$

and

$$\mathcal{H}_{h,i} = \frac{v_0}{2} C_i |\tilde{\Phi}(\mathbf{r}_{hi})|^2 \times \left(\frac{1}{2}(J_{h,+} I_{i,-}) + \frac{1}{2}(J_{h,-} I_{i,+}) + S_{e,z} I_{i,z} \right) \tag{5}$$

with the spin ladder operators $S_{e,\pm}$, $J_{h,\pm}$, and $I_{i,\pm}$. Flip-flop processes are initiated by the first two terms on the right-hand side.

An estimate of the resulting spin-flip rates can be obtained from lowest-order perturbation theory. Scattering between the two exciton populations is only possible when the energy difference of the exciton states coincides with the spin splitting of a nucleus, and hence the density of states of the nuclei plays an important role. Unfortunately this parameter is not known with high accuracy but can be at least estimated adequately. At first the nuclear splittings are broadened due to variations of the quadrupole momentum, and second a further broadening arises due to individually deviating magnetic surroundings in the dipole-dipole interaction. For simplicity we assume a uniform density of states that is unspecific with respect to the nuclei and their isotopes. The best agreement with the experimental relaxation times is obtained with all QD nuclei ($N \sim 8.5 \times 10^4$) spread over 75 neV. This value seems sensible since for (In,Ga)As/GaAs QDs the magnitude of the quadrupole interaction $h\nu_Q$ was estimated to be on the order of 1 to 10 neV, where ν_Q is the quadrupole frequency resulting from the electric field gradient at a given nuclear site with a certain strain.[36,37] Also the dipole-dipole interaction will further broaden the energy distribution of the nuclei. Especially central-spin mediated "co-flips" between nuclei involving a primary carrier spin might contribute here.[14,38] Choosing reasonable values for the remaining parameters describing the QD (details are given in the Appendix), the calculated spin relaxation times amount to 0.8 ns for an electron flip and 20 ns for a hole flip. Notably the ratio of these two times is in good agreement with our experimental results.

IV. CONCLUSIONS

We studied spin relaxations of excitons in InAs/GaAs QDs. In the undisturbed case the exchange interaction separates bright and dark exciton states energetically. Magnetic fields, however, drive the system into resonances where quasielastic spin scattering processes can take place. Two of such resonances are observed at each of which the lifetime of the involved dark exciton state is drastically shortened. Here a spin flip of either electron or hole occurs, converting the dark into a bright exciton. Due to the quasiresonant character we assign the origin of the underlying scattering process to the HF interaction. As we observe both electron and hole flips their spin dynamics can be compared for a single sample under comparable experimental conditions. The results show that spin flips involving an electron are approximately 25 times faster than those assisted by a hole flip. Our results are in agreement with previous studies on the HF interaction of QD-confined carriers where the HF interaction strengths of holes are found to be one order of magnitude smaller that those of the electrons.[17–19,24,25] A comparison with transition rates that are based on first-order perturbation theory verifies

our findings. With increasing temperature spin flips due to the SO interaction gradually become more important in the relaxation processes and finally dominate the exciton dynamics for $T > 30$ K.

ACKNOWLEDGMENTS

The support by the PlusLucis project, Ziel2.NRW program, and Deutsche Forschungsgemeinschaft (DFG 1549/10-1) is acknowledged. We thank J.-M. Chauveau, CNRS Valbonne, and A. Ludwig, Ruhr-Universität Bochum (now Department of Physics, University of Basel) for providing the TEM image.

APPENDIX: DETAILS OF THE MODELED EXCITON SPIN RELAXATION TIMES

The exciton evolution mentioned in Sec. III C is modeled by coupled rate equations where $M = +1$, -1, $+2$, and -2 excitons undergo spin flips or decay. The temperature-dependent spin relaxation between the bright and dark exciton population is described by the conversion time $\tau_{1\leftrightarrow 2}^{\text{fit}}$. Bright excitons decay with the above-mentioned $\tau_{\text{rad}} = 0.4$ ns obtained by time-resolved PL. The rate equation also assumes a phenomenological nonradiative decay channel for all excitons of $\tau_{\text{nonrad}} = 8$ ns which results together with $\tau_{1\leftrightarrow 2}^{\text{fit}}$ in the dark exciton decay rate ≈6 ns mentioned above for $T = 10$ K.

Assuming single-phonon scattering, the exciton spin relaxation times can be written according to Fermi's golden rule (FGR) as

$$\tau_{1\to 2}^{\text{FGR}} = \tau_0 (N+1)^{-1} \quad \text{and} \quad \tau_{2\to 1}^{\text{FGR}} = \tau_0 N^{-1},$$

where $N = [\exp(\delta_0/kT)]^{-1}$ is the phonon occupation factor for a given temperature T and exchange splitting δ_0, with k being the Boltzmann constant. All other underlying parameters are summarized in a zero-temperature relaxation time τ_0.[30,31] Together with the above-mentioned $\delta_0 = 100$ μeV, a value of $\tau_0 = 115$ ns was used.

TABLE I. Hyperfine constants and nuclear spin I.

Species	A_i (μeV)	C_i (μeV)	I
In	56	4.0	9/2
As	46	4.4	3/2
Ga	38	3.0	3/2

The transition rate for an initial state $|m\rangle$ into a final state $|n\rangle$ is $\Gamma_{mn} = \frac{2\pi}{\hbar}\varrho(E_n)|\langle n|\mathcal{H}_{e/h}|m\rangle|^2$, where $\varrho(E_n)$ is the density of the final states and $\mathcal{H}_{e/h}$ denotes the Hamiltonians above [Eqs. (4) and (5)]. The parameters for the numerical estimation of exciton spin flip times due to the HI interaction in Sec. III D are as follows: The number of unit cells is obtained via the QD volume. For the annealed QDs not enough contrast is obtained in electron microscopy to get reliable data on their geometry parameters. We assume a QD with a base diameter of 35 nm and a height of 8 nm [cf. the inset of an unannealed QD in Fig. 1(c)] and hence the modeled QD contains $\sim 8.5 \times 10^4$ nuclei. For reasons of simplicity the carriers are believed to be extended over the whole QD volume with a uniform probability. In order to consider material interdiffusion due to the RTA, a Ga intermixture of 0.42 is used. Usually the hole is located at the top of the QD, which is indium rich compared to the bottom, so that in this case a Ga intermixture of 0.18 was taken into account.[39] The In-, As-, and Ga-specific hyperfine constants as well as the nuclear spin I are given in Table I (values from Ref. 25). Clearly the spin relaxation rate for a hole depends strongly on the light-hole admixture β. $0.2 < |\beta| < 0.7$ were reported for strained dots.[40] For our calculations we use $|\beta| = 0.5$.

[1] *Spin Physics in Semiconductors*, edited by M. I. Dyakonov (Springer-Verlag, Berlin, 2008).
[2] A. V. Khaetskii and Y. V. Nazarov, Phys. Rev. B **61**, 12639 (2000); **64**, 125316 (2001).
[3] I. A. Merkulov, Al. L. Efros, and M. Rosen, Phys. Rev. B **65**, 205309 (2002).
[4] A. V. Khaetskii, D. Loss, and L. Glazman, Phys. Rev. Lett. **88**, 186802 (2002).
[5] W. A. Coish and D. Loss, Phys. Rev. B **70**, 195340 (2004).
[6] V. N. Golovach, A. Khaetskii, and D. Loss, Phys. Rev. Lett. **93**, 016601 (2004).
[7] J. R. Petta, A. C. Johnson, J. M. Taylor, E. A. Laird, A. Yacoby, M. D. Lukin, C. M. Marcus, M. P. Hanson, and A. C. Gossard, Science **309**, 2180 (2005).
[8] *Principles of Magnetic Resonance*, by C. P. Slichter (Springer-Verlag, Berlin, 1996).
[9] L. M. Woods, T. L. Reinecke, and Y. Lyanda-Geller, Phys. Rev. B **66**, 161318(R) (2002).
[10] M. Kroutvar, Y. Ducommun, D. Heiss, M. Bichler, D. Schuh, G. Abstreiter, and J. J. Finley, Nature (London) **432**, 81 (2004).
[11] D. Heiss, S. Schaeck, H. Huebl, M. Bichler, G. Abstreiter, J. J. Finley, D. V. Bulaev, and D. Loss, Phys. Rev. B **76**, 241306(R) (2007).
[12] P. F. Braun, X. Marie, L. Lombez, B. Urbaszek, T. Amand, P. Renucci, V. K. Kalevich, K. V. Kavokin, O. Krebs, P. Voisin, and Y. Masumoto, Phys. Rev. Lett. **94**, 116601 (2005).
[13] F. Fras, B. Eble, P. Desfonds, F. Bernardot, C. Testelin, M. Chamarro, A. Miard, and A. Lemaitre, Phys. Rev. B **84**, 125431 (2011).
[14] D. Gammon, A. L. Efros, T. A. Kennedy, M. Rosen, D. S. Katzer, D. Park, S. W. Brown, V. L. Korenev, and I. A. Merkulov, Phys. Rev. Lett. **86**, 5176 (2001).
[15] M. Paillard, X. Marie, P. Renucci, T. Amand, A. Jbeli, and J. M. Gérard, Phys. Rev. Lett. **86**, 1634 (2001).
[16] E. Tsitsishvili, R. V. Baltz, and H. Kalt, Phys. Rev. B **66**, 161405 (2002).
[17] E. A. Chekhovich, A. B. Krysa, M. S. Skolnick, and A. I. Tartakovskii, Phys. Rev. Lett. **106**, 027402 (2011).
[18] P. Fallahi, S. T. Yilmaz, and A. Imamoglu, Phys. Rev. Lett. **105**, 257402 (2010).

[19]J. Fischer, W. A. Coish, D. V. Bulaev, and D. Loss, Phys. Rev. B **78**, 155329 (2008).

[20]*Optical Orientation*, edited by F. Meier and B. P. Zakharchenya (North-Holland, Amsterdam, 1984).

[21]D. V. Bulaev and D. Loss, Phys. Rev. Lett. **95**, 076805 (2005); **98**, 097202 (2007).

[22]S. Laurent, B. Eble, O. Krebs, A. Lemaitre, B. Urbaszek, X. Marie, T. Amand, and P. Voisin, Phys. Rev. Lett. **94**, 147401 (2005).

[23]A. V. Koudinov, I. A. Akimov, Y. G. Kusrayev, and F. Henneberger, Phys. Rev. B **70**, 241305 (2004).

[24]B. Eble, C. Testelin, P. Desfonds, F. Bernardot, A. Balocchi, T. Amand, A. Miard, A. Lemaitre, X. Marie, and M. Chamarro, Phys. Rev. Lett. **102**, 146601 (2009).

[25]C. Testelin, F. Bernardot, B. Eble, and M. Chamarro, Phys. Rev. B **79**, 195440 (2009).

[26]M. Bayer, O. Stern, A. Kuther, and A. Forchel, Phys. Rev. B **61**, 7273 (2000).

[27]I. A. Yugova, A. Greilich, E. A. Zhukov, D. R. Yakovlev, M. Bayer, D. Reuter, and A. D. Wieck, Phys. Rev. B **75**, 195325 (2007).

[28]M. Bayer, A. Kuther, A. Forchel, A. Gorbunov, V. B. Timofeev, F. Schäfer, J. P. Reithmaier, T. L. Reinecke, and S. N. Walck, Phys. Rev. Lett. **82**, 1748 (1999).

[29]Spin flips within the bright or dark exciton reservoir are not of interest here since the latter ones are not relevant for the dark exciton lifetime shortening. Additionally such spin flips require relaxation processes of both electron and hole with a strongly reduced probability.

[30]E. Tsitsishvili, R. V. Baltz, and H. Kalt, Phys. Rev. B **67**, 205330 (2003); **72**, 155333 (2005).

[31]E. Tsitsishvili and H. Kalt, Phys. Rev. B **82**, 195315 (2010).

[32]P. San-Jose, G. Zarand, A. Shnirman, and G. Schön, Phys. Rev. Lett. **97**, 076803 (2006).

[33]M. Trif, P. Simon, and D. Loss, Phys. Rev. Lett. **103**, 106601 (2009).

[34]K. Roszak, P. Machnikowski, V. M. Axt, and T. Kuhn, Phys. Status Solidi C **6**, 537 (2009).

[35]The sample used in this work has a PL emission splitting of $\Delta E \approx 22$ meV (not shown). For holes the confinement energies are significantly (2 to 4 times) smaller than those of electrons. [See D. Reuter, P. Schafmeister, P. Kailuweit, and A. D. Wieck, Physica E **21**, 445 (2004); C. Bock, K. H. Schmidt, U. Kunz, S. Malzer, and G. H. Döhler, Appl. Phys. Lett. **82**, 2071 (2003).] Hence the energy separation between the ground state and excited states is likely around 5 meV for the holes.

[36]K. Flisinski, I. Ya. Gerlovin, I. V. Ignatiev, M. Yu. Petrov, S. Yu. Verbin, D. R. Yakovlev, D. Reuter, A. D. Wieck, and M. Bayer, Phys. Rev. B **82**, 081308 (2010).

[37]R. V. Cherbunin, K. Flisinski, I. Ya. Gerlovin, I. V. Ignatiev, M. S. Kuznetsova, M. Yu. Petrov, D. R. Yakovlev, D. Reuter, A. D. Wieck, and M. Bayer, Phys. Rev. B **84**, 041304 (2011).

[38]L. Cywinski, W. M. Witzel, and S. Das Sarma, Phys. Rev. Lett. **102**, 057601 (2009).

[39]P. W. Fry, I. E. Itskevich, D. J. Mowbray, M. S. Skolnick, J. J. Finley, J. A. Barker, E. P. O'Reilly, L. R. Wilson, I. A. Larkin, P. A. Maksym, M. Hopkinson, M. Al-Khafaji, J. P. R. David, A. G. Cullis, G. Hill, and J. C. Clark, Phys. Rev. Lett. **84**, 733 (2000); D. M. Bruls, J. W. A. M. Vugs, P. M. Koenraad, H. W. M. Salemink, J. H. Wolter, M. Hopkinson, M. S. Skolnick, Fei Long, and S. P. A. Gill, Appl. Phys. Lett. **81**, 1708 (2002).

[40]See, e.g., D. N. Krizhanovskii, A. Ebbens, A. I. Tartakovskii, F. Pulizzi, T. Wright, M. S. Skolnick, and M. Hopkinson, Phys. Rev. B **72**, 161312 (2005); T. Belhadj, T. Amand, A. Kunold, C.-M. Simon, T. Kuroda, M. Abbarchi, T. Mano, K. Sakoda, S. Kunz, and X. Marie, Appl. Phys. Lett. **97**, 051111 (2010).